38th International Electric Vehicle Symposium and Exhibition (EVS38) Göteborg, Sweden, June 15-18, 2025

Dynamic Optimization of EV Charging Based on Periodically Updated Battery RUL Algorithm

Josu Olmos[1], Unai Echeverria[1], Markel Azkue[1], Iñigo Gandiaga[1]

[1]*Ikerlan Technology Research Centre, Basque Research and Technology Alliance (BRTA), Pº J.M. Arizmendiarrieta 2, 20500 Arrasate/Mondragon, Spain.*
jolmos@ikerlan.es

Executive Summary

Precise battery Remaining Useful Life (RUL) algorithms are required to optimally design charging strategies for Electric Vehicles (EVs). However, the uncertainty of RUL estimations before EV commissioning is usually high, due to the scarce degradation evidence at that stage. To overcome this issue, data-driven RUL algorithms have been proposed, which can be periodically upgraded with real-life degradation evidence. These upgrades allow to regularly update any control strategy aiming to reduce battery degradation. In this context, this paper proposes a novel charging strategy for EVs, which is regularly optimized based on periodical updates of a data-driven RUL algorithm. The paper also introduces a simulation environment to demonstrate the strategy. The results demonstrate that regularly updating the charging strategy allows reaching a pre-defined battery end of life objective of 10 years with an error of 25 days, while a baseline strategy without updates may reach the end of life 2 years earlier.

Keywords: Electric Vehicles; Smart charging; Batteries; Battery Management System; AI – Artificial Intelligence for EVs

1 Introduction

Given the importance of lithium-ion Battery (BT) technology for the attainment of greenhouse gas emissions and global temperature increase reduction goals, it is necessary to continue advancing for a broader adoption of this technology. However, there are still some important drawbacks that hamper this wider adoption. Among others, high cost, short life cycle, constrained performance temperature, and possible safety infractions caused by overcharge, over-discharge, short circuit or even production defects are typically mentioned [1]. In some applications such as Electric Vehicles (EVs), some additional bottlenecks such as range anxiety or charging time are constantly mentioned in the literature [2], [3].

In the specific scope of BT charging, an inefficient strategy may result in the charging currents and voltages surpassing the BT tolerance limits, eventually leading to overheating, accelerated degradation, diminished longevity, and in the worst case, fires or explosions [4]. These challenges have been addressed in a wide amount of literature works, which explore diverse novel charging strategies for BT systems. Some comprehensive reviews about BT charging strategies can be found in the following references [1], [3], [5], [6]. These reviews classify charging strategies into passive methods (also referenced as non-feedback-based methods) and active methods (also referenced as feedback-based methods). In some cases, intelligent strategies are also considered as a separate category, but they can be also integrated into passive or active methods. Passive methods charge the BT under pre-set instructions, meaning that the charging is stopped when a certain condition is met, without varying the charging pattern based on the feedback of the BT [3]. Many of these works are focused on proposing variations of the traditional Constant Charge Constant Voltage (CC-CV) charging pattern: Multi-step CC (MCC), Multi-step CC with CV (MCC-CV), pulse charging, and negative pulse step after CC-CV (CC-CV-NP) are just some examples [7]. Besides, active methods charge the BT under dynamic profiles, which are adapted based on the feedback that the BT is providing [3]. This feedback can be provided directly by sensors, or by BT state estimators, e.g., State of Charge (SOC) or State of Health (SOH) estimators. Some

of the widely used active methods are based on predictive control, such as the Model Predictive Control (MPC) or the Generalized Predictive Control (GPC) [8], [9]. Optimization-based methods can be also categorized as active methods. Strategies based on Dynamic Programming (DP) or Pontryagin's Minimum Principle (PMP) are some examples that can be found in the literature [10], [11].

In the context of BT charging strategies, the degradation associated to the charging is one of the key points that directly impacts in the technical and economic viability of the application, especially in those where fast charging is preferred (e.g., in EVs). As the literature shows, there are different ways of addressing the minimization of the degradation associated to the BT charging. Some works consider the minimization of the degradation by just defining some constraints in the charging optimization problem. For instance, Jiang *et al.* [12] propose a Bayesian optimization to reduce the BT charging time, defining some temperature and voltage limits to reduce the BT ageing. Besides these simple approaches, other scientific works directly attain the extension of the BT lifetime as the main goal. Bharathraj *et al.* [13] propose a novel charging strategy based on dynamically adapting the charging cut-off voltage based on a physical model. This adaptation is triggered when the BT is reaching its End of Life (EOL), and the performed laboratory tests demonstrate a 30% extension on the BT lifetime. Besides, Lei *et al.* [14] propose a charging optimization method based on DP, being the objective the reduction of the energy loss and the degradation speed. An equivalent circuit model is employed to account for the lifetime evolution of the BT internal resistance, and an empirical degradation model is derived to evaluate the degradation associated to a specific charging pattern. Laboratory testing demonstrates that the degradation can be reduced a 33% with this method, but the conclusion is obtained after few testing cycles and capacity loss. Some other literature works directly consider the specific characteristics of the application in which the BT will be integrated. Hoke *et al.* [15] propose a charging optimization method that reduces the costs associated to the EV charging, considering not only the BT degradation, but also the varying electricity price at different time periods. For this aim, a degradation model that allows to directly assign an economical cost to a specific charging pattern is proposed. In short, the objective is to obtain an optimal trade-off between a lower BT degradation and charging at low electricity price periods. Another trend in the analyzed literature consists of finding or analyzing the optimal trade-off between the charging time and the associated degradation, as they are conflicting objectives. Lam *et al.* [16] propose an offline multi-objective optimization based on the single shooting framework to solve the mentioned trade-off, but they mainly focus on obtaining a robust controller. Besides, Appleton *et al.* [17] focus their contribution to comprehensively analyze the Pareto front possibilities of the mentioned trade-off problem. In order to derive the most appropriate solutions, they mainly focus on the limitations associated to the charging power and the cooling power. Some other similar approaches dealing with the mentioned trade-off can be found in [18], [19].

As it has been reviewed, many scientific works employ degradation models to estimate the degradation loss or degradation cost of a certain charging pattern, but they hardly estimate the lifetime associated to that charging pattern. Evaluating the Remaining Useful Life (RUL) can be an interesting solution to solve the trade-off between charging time and the associated degradation. Indeed, the BT integrator or BT manufacturer may be interested on reaching a specific BT EOL, as the whole system may have been optimally designed based on the assumption of a specific lifetime threshold. In order to implement this approach, a RUL estimation algorithm is necessary [20]. One of the main limitations of RUL algorithms is the high uncertainty of the estimations when the BT has not been yet tested in real life, as the degradation patterns significantly differ from laboratory conditions to real operation. Consequently, the uncertainty of the charging strategies designed before EV commissioning might be also high. In order to overcome the low precision of degradation estimation before commissioning, data-driven RUL algorithms oriented to be updated with real-life data have been proposed in the literature [21]. Updating the RUL algorithm through the BT lifetime also allows to update on a regular basis any control strategy aiming to reduce the BT degradation, including the charging strategy.

In this context, this paper proposes a novel charging strategy for EVs, which is regularly optimized based on the periodical updates of a data-driven RUL estimation algorithm. To the best of the author's knowledge, these are the main contributions of the present paper:

1. The trade-off between charging time and BT degradation is proposed to be solved in terms of EOL, i.e., the optimal charging strategy is defined as the charging patter that gets closer to a specific and pre-determined EOL.
2. In order to counteract the uncertainty of RUL estimation models, regular updates of the model are proposed during the BT lifetime. This allows to periodically find a new optimal trade-off between charging time and BT degradation, and therefore, to better adjust to the pre-determined EOL.

The remainder of the paper is structured as follows. Section 2 details the RUL algorithm implemented together with the novel charging algorithm. Then, Section 3 derives the periodically optimized charging strategy. Section 4 focuses on the environment proposed to demonstrate the concept of the novel charging strategy, and Section 5 presents the Case Study selected for the even objective. Hereafter, in Section 6 the obtained results are presented, and a discussion on these results is derived. Finally, Section 6 reviews the main conclusions and outlines the future lines of the proposed work.

2 Remaining Useful Life (RUL) Estimation Algorithm

As derived in Section 1, the novel charging algorithm proposed in this paper is based on the predictions made by a RUL algorithm. As different reviews show, the development of a RUL algorithm for BTs is a widely addressed research topic in the literature [22], [23], [24]. Deriving a novel RUL algorithm stays out of the scope of the current research work, and therefore the data-driven ageing algorithm proposed by Lucu *et al.* is implemented [21], [25], [26]. This section gives a general overview of this algorithm in order to understand how it is implemented together with the proposed charging strategy. First, the theoretical basis of the ageing model is given in Section 2.1. Then, the processes carried out to re-train the model and perform predictions based on field data are derived in Sections 2.2 and 2.3, respectively.

2.1 Theoretical Background

The data-driven ageing model implemented in this paper is based on the Gaussian Process (GP) framework [27]. The GP model was selected due to its nonparametic and probabilistic features – it has the increased capability of integrating new information from the data collected in-field, and it allows to evaluate the reliability of the model's predictions, respectively [21]. The GP is a random process, i.e. a random entity whose realization is a function $f(x)$ instead of a single value. The GP is fully determined by its mean and covariance functions, which encodes the prior assumptions about the function to be learnt. Eqs. (1)-(3) summarize the GP definition, being $m(x)$ the mean function, $k(x, x')$ the kernel function, and x and x' two different input vectors. The reader is referred to the book written by Rasmussen and Williams for a broader theoretical and mathematical derivation of the GP framework [27].

$$f(x) \sim \mathcal{GP}(m(x), \kappa(x, x')) \tag{1}$$

$$m(x) = \mathbb{E}[f(x)] \tag{2}$$

$$\kappa(x, x') = \left[\left(f(x) - m(x)\right)\left(f\left(x'\right) - m\left(x'\right)\right)\right] \tag{3}$$

The RUL algorithm is composed of: (1) a first GP model that predicts the capacity loss when the BT is under calendar conditions, i.e., when the BT is not operating; and (2) a second GP model that predicts the capacity loss under cycling conditions, i.e., when the BT is operating.

On the one hand, the calendar model considers as inputs: (1) the storage time [days] since the BT Beginning of Life (BOL), (2) the storage time [days] experienced by the cell and for which the ageing is desired to be predicted, (3) the temperature [K] corresponding to this storage time, and (4) the SOC level [%] corresponding to this storage time. According to this input variables, the corresponding capacity loss [%] of the BT is predicted as output. The detailed development and validation of the calendar GP model is found in [26].

On the other hand, the cycling model considers as input: (1) the number of Full Equivalent Cycles (FEC) [#] that the BT has cycled since BOL, (2) the amount of FEC [#] experienced by the cell and for which the ageing is desired to be predicted, (3) the temperature [K] corresponding to the cycled FEC, (4) the Depth of Discharge (DOD) level [%] corresponding to the cycled FEC, (5) the average SOC [%] corresponding to the cycled FEC, (6) the charging C-rate [h^{-1}] corresponding to the cycled FEC, and (7) the discharging C-rate [h^{-1}] corresponding to the cycled FEC. According to this input variables, the corresponding capacity loss [%] of the BT is predicted as output. The detailed development and validation of the cycling GP model is found in [25].

Therefore, concatenating sequential predictions of the calendar and cycling operation, it is possible to derive the remaining time until the capacity of the BT drops below the defined EOL, i.e., the RUL prediction.

2.2 RUL Training based on Field Data

Typically, BT operation data collected in-field is represented in terms of current, voltage and temperature time series. Systems with advanced Battery Management System (BMS) functionalities may also include regular

SOC and SOH estimations. In any case, the data collected in-field requires a processing step in order to obtain the appropriate data structure for the periodical trainings of the calendar and cycling models during the BT lifetime (which are required for the charging strategy updates).

The data processing step includes a target processing algorithm (required to obtain the model output) and an input processing algorithm (required to obtain the model inputs), as illustrated in Figure 1. Both algorithms are applied through the data collected in an observation period. Two consecutive observation period may have different length, but they should not be overlapped. The generated new training matrix should be attached to the already existing matrixes, also to the ones that were not generated from field data. Both target and input processing algorithms are further derived in the following sub-sections.

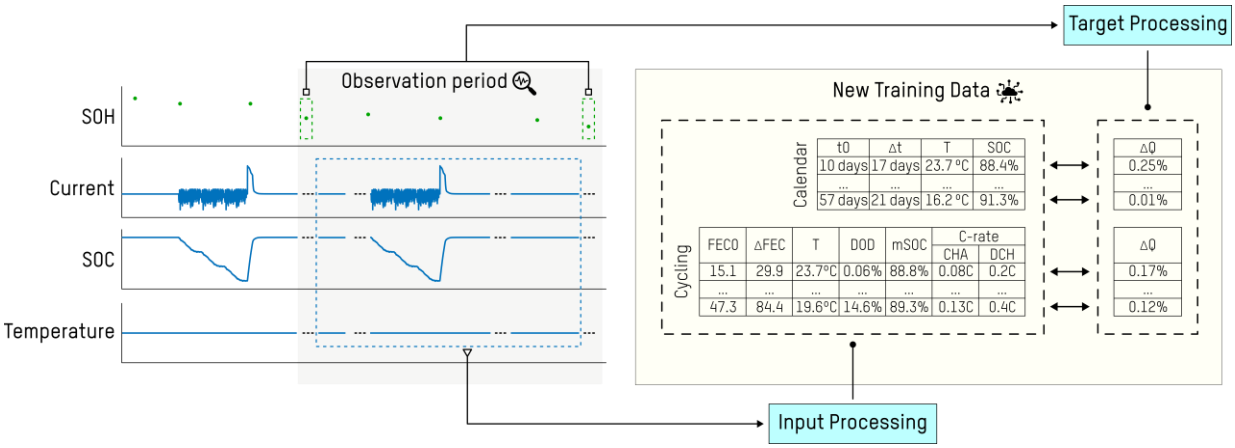

Figure 1: Method for the extraction of training data from field data. Adapted from [21].

2.2.1 Target Processing Algorithm

The target processing algorithm aims at deriving the capacity loss required by the ageing model for the training. The capacity loss is derived based on the SOH estimation provided by the BMS. During field operation, BTs are typically subjected to both calendar and cycling operation taking place successively. Besides, the periodical SOH estimations are not necessarily carried out at every transition between calendar and cycling phases, as no significant ageing may be experienced in such short-term. For these reasons, the SOH loss data computed during an observation period must be split and associated with the sequential calendar and cycling operating conditions experienced between them, as depicted in Figure 1.

This process is composed of the following steps [21]: (1) the overall SOH loss data is decomposed into a calendar and cycle components, applying a decomposition factor based on the respective duration of the calendar and cycling phases with respect to the total duration of the observation period, (2) the calendar capacity loss component is partitioned among each input vector of the calendar ageing model training data (obtained from the input processing algorithm, see Section 2.2.2), applying a decomposition factor based on the respective duration of each vector with respect of the total duration of the calendar phase; and (3) the cycle capacity loss component is partitioned among each input vector of the cycle ageing model training data (also obtained from the input processing algorithm, see Section 2.2.2), applying a decomposition factor that in this case is based on the number of FECs of each vector with respect of the total FECs of the cycling phase.

2.2.2 Input Processing Algorithm

The starting point of the input processing algorithm is the decomposition of the current, temperature and SOC time series, which eventually derive to the calendar and cycling components of the BT operation. This decomposition starts with a zero-current detection step, which allows defining the calendar sections of the observation period. A minimum length of 60 seconds without current is required for the definition of a calendar step. Once the cycling and calendar sections are divided, they are processed separately.

In the case of the cycling operation, the following steps are followed [21]: (1) from the current time series, positive and negative half-cycles are distinguished; (2) for each half-cycle, and based on the current, temperature and SOC time series, the average values of the temperature, DOD, middle SOC, and charging and discharging C-rates are calculated; (3) the number of FECs cycled at similar stress-factor values are accumulated, separately for the charging and discharging half-cycles; and (4) the accumulated charging and discharging half-cycles corresponding to similar temperature, DOD and middle SOC are associated to

synthesize full-cycles. In this way, input vectors are generated and organized in a design matrix for the cycling ageing model, as previously depicted in Figure 1.

In parallel, the sections of the current, temperature and SOC time series that were assigned to the calendar operation are also processed, in order to generate an analogue input table for the calendar ageing model, consistent with the data structure previously described in Section 2.1.

2.3 RUL Predictions based on Field or Predicted Data

Performing a RUL prediction requires to define the future BT operation, and this can be carried out based on the past field data or based on estimations of the future operation (e.g., with operation prediction algorithms). Regardless of this definition, a processing step might be necessary before performing a RUL prediction to adapt the voltage, current, temperature and SOC time series to the appropriate data structure, analogously to the approach necessary to define the training data. In this case, only the input processing algorithm derived in Section 2.2.2 is required.

3 Periodically Optimized Charging Strategy

This section derives in detail the periodically updated charging strategy proposed in this paper. Essentially, the proposed concept can be implemented with many of the charging patterns reviewed in Section 1 – CC-CV, MCC, model-based or even optimization methods. However, the strategy proposed in this paper is oriented to be integrated in a BMS. These devices just provide in real time the maximum power or current that the BT can withstand, as they do not actively act on the BT charging current. Another controller (typically a DC/DC converter associated to the BT) reads this maximum allowable current value from the BMS and eventually fixes the BT current based on that reading. Indeed, some of the advanced charging algorithms reviewed in Section 1 should be embedded in these controllers, due to the limiting set of actions that the BMS can perform. Consequently, in this paper a baseline strategy based on the typical CC charging protocol is defined. The charging strategy will be just in charge of defining in real time the maximum charging current value that the BMS will issue (I_{ch-max}). Having the charging strategy associated to a specific BMS allows to perform the periodical optimizations based on the historical use of that specific BT, contrary to the case where the strategy is embedded in the controller.

In this context, the periodical optimizations proposed as main contribution of this paper adapt the maximum charging current value based on the estimations of the updated RUL algorithm (see Section 2). As previously explained, this approach allows to obtain an appropriate trade-off between charging rates that may damage too fast the BT and charging rates that may be too conservative. Besides these periodical updates, the proposed strategy should also reduce the impact of non-safe BT operation conditions during EV charging, which is performed based on the real-time information collected by the BMS (mainly, temperature and voltage measurements). Due to the different time scale of the two tasks to be performed by the charging strategy, the proposed novel concept is divided into two levels, denoted as Level-1 and Level-2, as depicted in Figure 2.

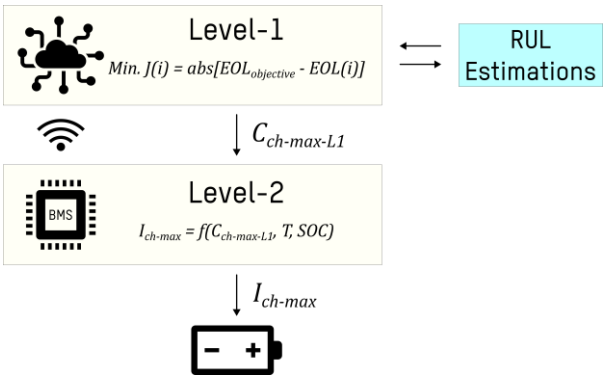

Figure 2: General overview of proposed charging algorithm.

On the one hand, Level-1 is oriented to define the maximum BT charging current that better adjusts to a specific EOL objective. Due to the complex operations and the high computational effort required, Level-1 needs to be deployed in a cloud system that extends the capabilities of the low-level traditional BMS. The RUL estimation algorithm should also be integrated in the mentioned cloud system. On the other hand, Level-2 is executed in the low-level BMS, and consists of a derating factor that reduces the maximum charging current value of Level-1 according to the instantaneous BMS measurements. Eventually, the maximum current value provided

by the Level-2 is the value that the BMS issues.

It is worth mentioning that the multi-layer BMS architecture (including the low-level and cloud layers) required to deploy the proposed strategy is being developed in BIG LEAP project [28]. BIG LEAP is a Horizon Europe initiative that aims at improving the reliability of second-life BTs by addressing interoperability in BMSs and Energy Storage Systems (ESS).

3.1 Level-1 Charging Algorithm

Level-1 deploys an optimization based on an exhaustive search. Specifically, a set of possible maximum charging C-rates (C_{ch}) is defined, and the remaining life of the BT under each C_{ch} value is predicted with the RUL algorithm presented in Section 2. Then, the C_{ch} value that obtains the RUL value closest to a predefined EOL objective is defined as the optimal charging pattern.

In order to perform the optimization, Level-1 first initializes the exhaustive search optimization. For that aim, a set of potential C_{ch} values is defined, noted as I. As mayor discretization, a more precise optimization result is obtained, but more loops and execution time is required. Once the initialization is ready, the optimization loops are executed. At each loop a potential C_{ch} value is evaluated (i), and the same 3 steps are followed:

1. The first step consists of defining the necessary input for the RUL estimation. As explained in Section 2, this requires estimating the future BT operation under the considered C_{ch} value. Considering the random nature of EV driving patterns, and that optimizing the driving pattern itself stays out of the scope of the proposed optimization, it is not considered feasible nor necessary to derive an estimator for the future driving cycles. Instead of this approach, the future BT operation is based on the collected past data. Specifically, the data input matrixes (see Figure 1) collected during the year prior to the optimization are used as reference. Only the "C-rate CHA" column is modified – the values are proportionally modified according to the C_{ch} value being evaluated, and in relation to the maximum C_{ch} limitation applied during that specific time.
2. The RUL algorithm presented in Section 2 is triggered to estimate the remaining life under the considered future BT operation.
3. The optimization cost $J(i)$ is computed, following equation (4). The equation requires defining beforehand the EOL objective for the BT ($EOL_{objective}$). This value might be defined as the warranty period of the BT defined by the manufacturer.

$$J(i) = abs[EOL_{objective} - EOL(i)] \quad (4)$$

Finally, the C_{ch} value with the lowest cost function is defined as the optimal charging pattern, $C_{ch-max-L1}$. Each time the optimization is performed, the obtained $C_{ch-max-L1}$ value is sent to the low-level BMS, where it is used as reference point for the Level-2 charging algorithm.

3.2 Level-2 Charging Algorithm

In order to meet together the real time and safety requirements, Level-2 is based on a derating strategy that reduces the $C_{ch-max-L1}$ value defined in Level-1 according to the instantaneous BT temperature and SOC. This strategy is typically adopted by BMS or BT manufacturers, and consists of the combination of two individual derating vectors, which are defined individually for temperature and SOC. The definite derating factor (and consequently, the maximum current I_{ch-max}) is calculated as the multiplication of the two derating factors (d_T and d_{SOC}), as shown in Eq. (5). Figure 3 shows the concrete values of the individual derating vectors implemented in this paper. As depicted, a smooth transition between the different states is proposed.

$$I_{ch-max} = C_{ch-max-L1} \cdot d_T \cdot d_{SOC} \quad (5)$$

4 Simulation Environment

This section presents the simulation environment implemented in this paper for the demonstration of the proposed charging concept. Indeed, this simulation environment is necessary to estimate the operation of the BT under different charging conditions, and also to estimate the associated degradation. Figure 4 shows the general scheme of this environment, which consists of the main 4 steps highlighted in the figure itself. These steps are detailed below. It is worth noting that these steps do not need to be executed always in a sequential order, as they can be triggered with different frequencies.

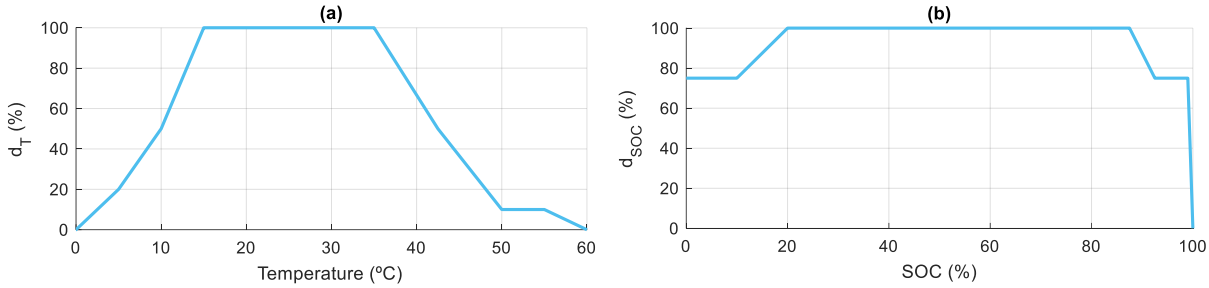

Figure 3: Derating factors for Level-2: a) d_T b) d_{SOC}.

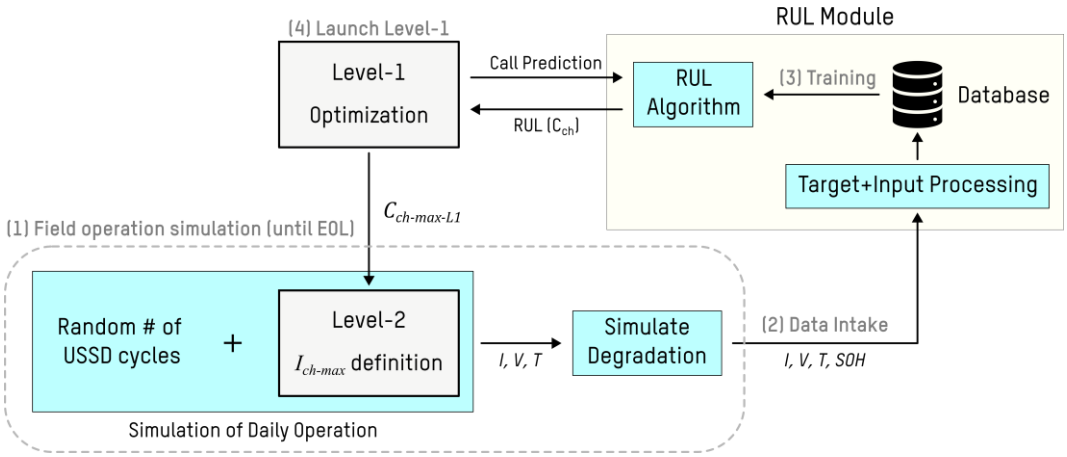

Figure 4: Simulation framework for the demonstration of the charging concept.

The first step consists of the EV field operation simulation, which is an iterative process that continuously simulates the daily BT operation and estimates the associated BT ageing. The daily simulation consists of concatenating a random EV operation with a charging operation right after the operation is finalized. During the EV operation, a random number of driving cycles is concatenated, with the aim of representing a user with random EV usage. The driving cycles are based on the UDDS profile and consist of the measurements available in the dataset by Pozzato *et al.* [29]. The random number of repetitions is generated via a Gaussian distribution with $\mu = 0$ and $\sigma^2 = 4$, converting the negative values to positive ones. To avoid a discharge below 20% SOC, no more than 8 repetitions can be concatenated. During the EV charge, the BT is charged until the 100% SOC with the value issued by Level-2, I_{ch-max}.

After each daily simulation, the associated BT degradation is computed. The SOH value of the BT is updated according to a simplification of the model proposed by Olmos *et al.* in [30]. Specifically, expression in Eq. (6) is applied, which defines the SOH loss at the current time step. In the expression, i represents the current time step, T the battery temperature, C_{ch} the charging C-rate, C_{dch} the discharging C-rate, and $\beta, k_T, T_{ref}, k_{Cch}, k_{Cdch}$ and α are model parameters (specified in Section 5).

$$dSOH_i = \beta \cdot exp\left(k_T \cdot \frac{T - T_{ref}}{T} + k_{Cch} \cdot C_{ch} + k_{Cdch} \cdot C_{dch}\right) \cdot (FEC_i^{\alpha} - FEC_{i-1}^{\alpha}) \quad (6)$$

The second step of the simulation framework is the data intake process. This step represents the compilation of the raw operation data of the BT, and the execution of the data processing step explained in Section 2.2. The data intake is tackled with a fixed frequency (i.e., it is not a continuous daily process), mainly with the aim of obtaining a data slot with a representative SOH loss. Finally, the two last steps of the simulation framework are the training of the RUL algorithm (according to the model represented in Section 2.1 and 2.2), and the execution of the Level-1 optimization based on the updated RUL model (based on the method presented in Section 3.1).

5 Case Study

This section presents the selected case study for the demonstration of the proposed charging concept, which will be evaluated in the simulation framework previously presented in Section 4.

A representative BT system has been selected for the case study, whose main details are depicted in Table 1.

The module is based on the cell cycled in the dataset by Pozzato *et al.* [29]. Indeed, the current, voltage and temperature time-series included in this dataset have been used to simulate the BT operation.

Variable	Value
Chemistry	NMC
Capacity	4.85 Ah
Voltage Range	30 - 50.4 V
Continuous ch/dch C-rate	2C/2C
Design Lifetime	10 years

Table 1: Representative data of defined BT module.

Considering the chemistry of the selected BT and its design lifetime, the parameters of the model implemented to estimate the BT ageing (see Section 4) have been adapted from the original model [30]. Table 2 shows the updated parameters.

Parameter	Value
β	0.019827
k_T	11.62
k_{Cch}	0.5898
k_{Cdch}	0.1077
T_{ref}	293.15
α	0.91

Table 2: Parameters of BT ageing model used to estimate SOH evolution.

Eventually, Table 3 defines the set of parameters required for the execution of Level-1. $EOL_{objective}$ is defined at 10 years, in accordance with the normal lifetime design. Initially, $C_{ch-max-L1}$ is defined at 2C, and after 6 months of operation, the first Level-1 OCA is executed. The frequency of RUL training is also defined at 6 months, while the frequency for the data intake (and data processing) is defined at 3 months.

Parameter	Value
$EOL_{objective}$	10 years
EOL critera	80% SOH
Initial $C_{ch-max-L1}$	2C
C_{ch} value set (I)	[0.25, 0.5, 0.75, 1, 1.25, 1.5, 1.75, 2]
Frequency of data intake	3 months
Frequency of RUL training	6 months
Frequency of Level-1	6 months

Table 3: Configuration of Level-1 optimization.

6 Results and Discussion

This section presents the results of the proposed charging strategy, which has been simulated in the framework defined in Section 4, according to the case study defined in Section 5. Figure 5 shows the summary of the obtained results, specifically, in terms of SOH evolution. The figure depicts the following information:

- The discontinuous light blue line represents the linear degradation trend to reach the defined EOL objective (20% SOH loss after 10 years), i.e., it represents the aimed degradation trend.
- The continuous dark blue line represents the final degradation curve of the BT obtained in simulation, i.e., after applying the charging updates. In order to obtain an effective charging strategy, the dark blue line should follow as close as possible the light blue line.
- The discontinuous red and green lines represent the two worst cases of the optimization problem, i.e., a case in which the maximum C-rate is always defined at 2C (red line), and a case in which the maximum C-rate is always defined at 0.25C (green line). It is worth noting that due to the random nature of the simulated driving cycles, two simulations with the same maximum C-rate may not obtain the same exact degradation evolution.
- The values above the arrows at the top of the figure represent the maximum charging C-rate allowed at each time frame ($C_{ch-max-L1}$), i.e., the results returned by the periodical Level-1 optimizations.

The exact values returned at each optimization are shown in Table 4.

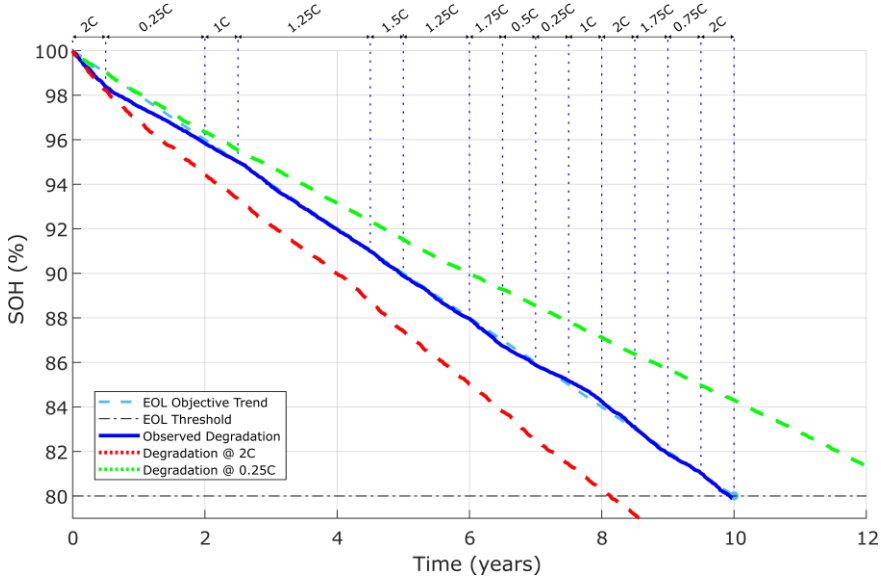

Figure 5: Results of the BT ageing evolution with the proposed charging strategy.

Time	Optimization Result	Time	Optimization Result
Year 0	-	Year 5	1.25 C
Year 0.5	0.25 C	Year 5.5	1.25 C
Year 1	0.25 C	Year 6	1.75 C
Year 1.5	0.25 C	Year 6.5	0.5 C
Year 2	1 C	Year 7	0.25 C
Year 2.5	1.25 C	Year 7.5	1 C
Year 3	1.25 C	Year 8	2 C
Year 3.5	1.25 C	Year 8.5	1.75 C
Year 4	1.25 C	Year 9	0.75 C
Year 4.5	1.5 C	Year 9.5	2 C

Table 4: Results returned by Level-1 optimization.

The results show that the battery reaches the EOL at 9.93 years, 25 days prior to the defined EOL objective (10 years). This means that an absolute error of the 0.7% is obtained. This can be denoted as an appropriate result, even if the EOLs obtained at the two worst cases are considered – with a continuous 2C charge, the EOL is reduced to 8.13 years (1.8 years less than the obtained EOL); while with a continuous 0.25C charge, the EOL can be extended to 12.9 years (2.97 years more than the obtained EOL). Therefore, even if only the feasible EOL window is considered (difference between the EOLs derived at 2C and 0.25C), the obtained deviation leads to a relative error of the 1.47% (0.07 years deviation in relation to 4.93 years of feasible window). The error in relation to the feasible EOL window is also relevant, as the obtained absolute error depends on the ageing model implemented in the proposed case study (see Table 2). Even in an excessive case with a feasible EOL window of 16 years (e.g., the EOL with the hardest charging leads to 2 years of lifetime, and the EOL with the softest charging leads to 18 years), the obtained relative error would derive into an EOL of 9.76 years (absolute error of the 2.3%).

Looking with more detail into the yearly evolution of the degradation curve, it can be noted that the main deviation is obtained at the first half year, when the initial maximum charging C-rate is defined at 2C (without deploying the Level-1 optimization). Then, in the first optimization, the Level-1 OCA identifies the deviation, and proposes a 0.25C maximum charge to reduce the gap with the ideal trend. This proposal is maintained for 1.5 years, until the realistic degradation curve (dark blue) gets closer to the ideal degradation curve (light blue). Then, for 4 years, the maximum C-rate proposal gets quite stable between 1 and 1.5C, and the realistic curve follows approximately the ideal curve. From year 6 on, it can be noted that the Level-1 OCA gets more unstable, as it changes the maximum allowable C-rate each time the execution is launched. In any case, during the remaining 4 years, even if at same points the realistic curve deviates from the ideal curve, the overall trend leads to an EOL close to the defined objective, as previously highlighted.

Figure 6 shows some examples of the optimization carried out at specific moments during the battery lifetime. Specifically, the RUL predictions performed at year 0.5 (first optimization), year 4 and year 7.5 are depicted. It can be noted that the difference between the proposed maximum C-rates is not very high, contrary to the difference identified in the realistic degradation (difference between green and red lines in Figure 28). The RUL algorithm is able to predict better this difference when more realistic data is observed (note that the difference in the RUL predictions is higher at year 4 compared to year 0.5), but this is not enough to reach the same trend as the observed realistic degradation. In any case, even with the identified limitation, the continuous optimization process allows getting a final EOL close to the predefined objective, as previously highlighted. This demonstrates that the proposed charging concept does not necessitate a very accurate RUL estimator, as the proposed updates allow to counteract this limitation.

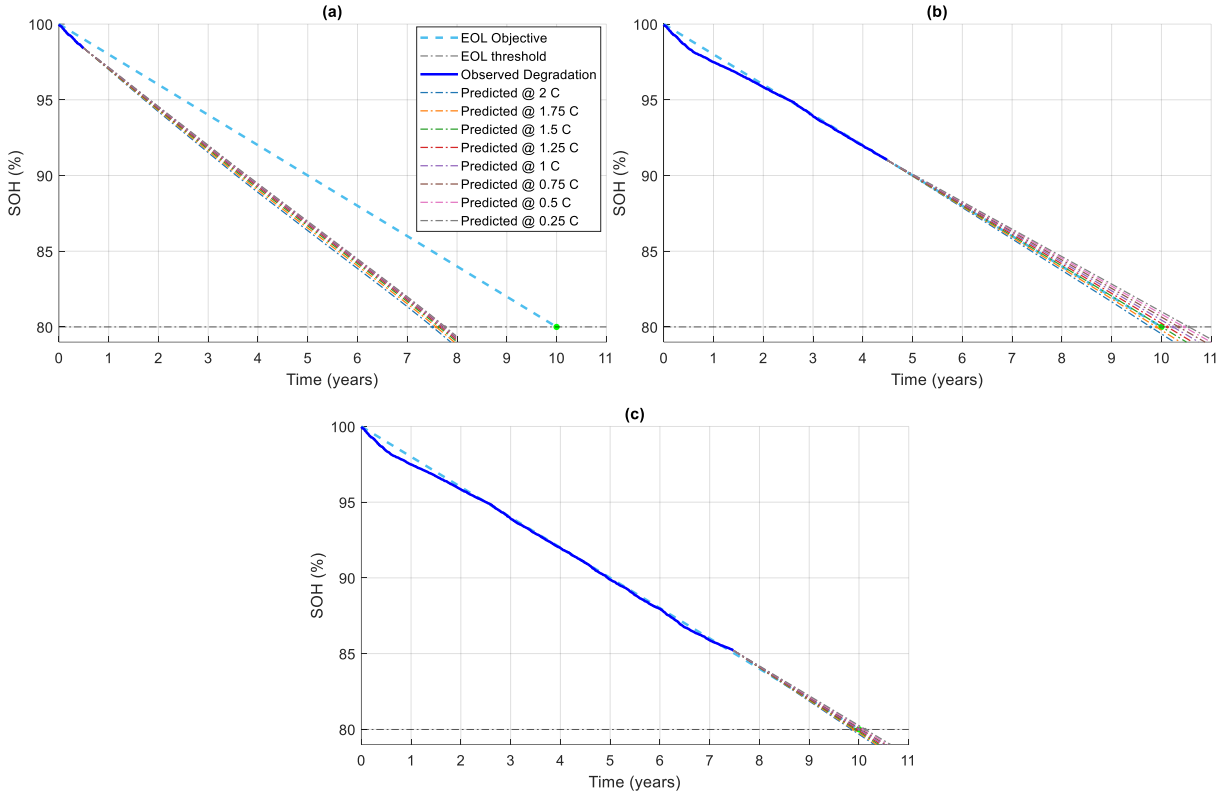

Figure 6: Examples of Level-1 optimization: a) at 0.5 years, b) at 4 years, c) at 7.5 years.

7 Conclusions and Future Lines

This paper has presented a novel concept for EV charging optimization, which is based on updating the charging pattern based on the periodical updates of a data-driven RUL estimation algorithm. The two main contributions of the proposed concept are claimed to be: 1) The trade-off between charging time and BT degradation is solved in terms of EOL, and 2) regular updates of the RUL estimation model are proposed during the BT lifetime, in order to counteract the uncertainty of the model itself, and allowing to periodically find a new optimal trade-of between charging time and BT degradation.

The obtained results have demonstrated the benefits of both contributions. On the one hand, it is considered that an appropriate trade-off between charging time and BT degradation has been obtained in the simulated case study. Indeed, the BT follows the predefined degradation objective with an error at EOL of just 0.07 years (0.7% absolute error). The error has been demonstrated to be low even if only the feasible EOL window is considered), what demonstrates that the BT would also follow the predefined degradation trend in a scenario where the degradation differs more between the proposed charging C-rates. On the other hand, the benefit of the periodical updates has also been demonstrated. Indeed, it has been noted that the RUL algorithm is not able to perfectly predict the difference in degradation between the proposed charging patterns. These estimations are improved as more data is collected from field operation, but it is not enough to perfectly predict the realistic trends. In any case, even with these limitations, the proposed updates allow the degradation evolution to not deviate from the predefined objective, what demonstrates the benefits of the proposed charging concept.

Future lines of this work include the deploying of the charging concept in a real BT demonstrator with a cloud monitoring platform, what would allow to demonstrate the concept in a real-life application. Moreover, another research line derived from the current work may include the coupling of the proposed Level-1 optimization with an improved Level-2, which would be optimized in real-time to improve the thermal behavior of the BT.

Acknowledgments

This work has been developed in the framework of the BIG LEAP project, co-funded by the European Union under grant agreement Nº101137815.

References

[1] N. Ghaeminezhad and M. Monfared, "Charging control strategies for lithium-ion battery packs: Review and recent developments," *IET Power Electronics*, vol. 15, no. 5, pp. 349–367, Apr. 2022, doi: 10.1049/pel2.12219.

[2] B. Bose, A. Garg, B. K. Panigrahi, and J. Kim, "Study on Li-ion battery fast charging strategies: Review, challenges and proposed charging framework," *J Energy Storage*, vol. 55, p. 105507, Nov. 2022, doi: 10.1016/j.est.2022.105507.

[3] Y. Gao, X. Zhang, Q. Cheng, B. Guo, and J. Yang, "Classification and Review of the Charging Strategies for Commercial Lithium-Ion Batteries," *IEEE Access*, vol. 7, pp. 43511–43524, 2019, doi: 10.1109/ACCESS.2019.2906117.

[4] G. Ji, L. He, T. Wu, and G. Cui, "The design of fast charging strategy for lithium-ion batteries and intelligent application: A comprehensive review," *Appl Energy*, vol. 377, p. 124538, Jan. 2025, doi: 10.1016/j.apenergy.2024.124538.

[5] B. Arabsalmanabadi, N. Tashakor, A. Javadi, and K. Al-Haddad, "Charging Techniques in Lithium-Ion Battery Charger: Review and New Solution," in *IECON 2018 - 44th Annual Conference of the IEEE Industrial Electronics Society*, IEEE, Oct. 2018, pp. 5731–5738. doi: 10.1109/IECON.2018.8591173.

[6] A. Tomaszewska *et al.*, "Lithium-ion battery fast charging: A review," *eTransportation*, vol. 1, p. 100011, Aug. 2019, doi: 10.1016/j.etran.2019.100011.

[7] B. Bose, S. Shaosen, W. Li, L. Gao, K. Wei, and A. Garg, "Cloud-Battery management system based health-aware battery fast charging architecture using error-correction strategy for electric vehicles," *Sustainable Energy, Grids and Networks*, vol. 36, p. 101197, Dec. 2023, doi: 10.1016/j.segan.2023.101197.

[8] K. Liu, K. Li, and C. Zhang, "Constrained generalized predictive control of battery charging process based on a coupled thermoelectric model," *J Power Sources*, vol. 347, pp. 145–158, Apr. 2017, doi: 10.1016/j.jpowsour.2017.02.039.

[9] C. Zou, X. Hu, Z. Wei, T. Wik, and B. Egardt, "Electrochemical Estimation and Control for Lithium-Ion Battery Health-Aware Fast Charging," *IEEE Transactions on Industrial Electronics*, vol. 65, no. 8, pp. 6635–6645, Aug. 2018, doi: 10.1109/TIE.2017.2772154.

[10] S. Pramanik and S. Anwar, "Electrochemical model based charge optimization for lithium-ion batteries," *J Power Sources*, vol. 313, pp. 164–177, May 2016, doi: 10.1016/j.jpowsour.2016.01.096.

[11] X. Lin, X. Hao, Z. Liu, and W. Jia, "Health conscious fast charging of Li-ion batteries via a single particle model with aging mechanisms," *J Power Sources*, vol. 400, pp. 305–316, Oct. 2018, doi: 10.1016/j.jpowsour.2018.08.030.

[12] B. Jiang *et al.*, "Fast charging design for Lithium-ion batteries via Bayesian optimization," *Appl Energy*, vol. 307, p. 118244, Feb. 2022, doi: 10.1016/j.apenergy.2021.118244.

[13] S. Bharathraj, S. P. Adiga, K. S. Mayya, T. Song, J. Kim, and Y. Sung, "Degradation-guided optimization of charging protocol for cycle life enhancement of Li-ion batteries with Lithium Manganese Oxide-based cathodes," *J Power Sources*, vol. 474, p. 228659, Oct. 2020, doi: 10.1016/j.jpowsour.2020.228659.

[14] Y. Lei, C. Zhang, Y. Gao, and T. Li, "Charging Optimization of Lithium-ion Batteries Based on Capacity Degradation Speed and Energy Loss," *Energy Procedia*, vol. 152, pp. 544–549, Oct. 2018, doi: 10.1016/j.egypro.2018.09.208.

[15] A. Hoke, A. Brissette, K. Smith, A. Pratt, and D. Maksimovic, "Accounting for Lithium-Ion Battery Degradation in Electric Vehicle Charging Optimization," *IEEE J Emerg Sel Top Power Electron*, vol. 2, no. 3, pp. 691–700, Sep. 2014, doi: 10.1109/JESTPE.2014.2315961.

[16] F. Lam, A. Allam, W. T. Joe, Y. Choi, and S. Onori, "Offline Multiobjective Optimization for Fast Charging and Reduced Degradation in Lithium-Ion Battery Cells Using Electrochemical Dynamics,"

IEEE Control Syst Lett, vol. 5, no. 6, pp. 2066–2071, Dec. 2021, doi: 10.1109/LCSYS.2020.3046378.
[17] S. Appleton and A. Fotouhi, "A Model-Based Battery Charging Optimization Framework for Proper Trade-offs Between Time and Degradation," *Automotive Innovation*, vol. 6, no. 2, pp. 204–219, May 2023, doi: 10.1007/s42154-023-00221-8.
[18] Z. Salyer, M. D'Arpino, M. Canova, and Y. Guezennec, "Optimal Health-Conscious Fast Charging of Lithium Ion Batteries," in *IFAC-PapersOnLine*, Elsevier B.V., Nov. 2021, pp. 516–521. doi: 10.1016/j.ifacol.2021.11.224.
[19] M. Kim and J. Kim, "Advanced Integrated Fast-Charging Protocol for Lithium-Ion Batteries by Considering Degradation," *ACS Sustain Chem Eng*, vol. 12, no. 17, pp. 6786–6796, Apr. 2024, doi: 10.1021/acssuschemeng.4c01673.
[20] S. Ansari, A. Ayob, M. S. Hossain Lipu, A. Hussain, and M. H. M. Saad, "Remaining useful life prediction for lithium-ion battery storage system: A comprehensive review of methods, key factors, issues and future outlook," Nov. 01, 2022, *Elsevier Ltd*. doi: 10.1016/j.egyr.2022.09.043.
[21] M. Lucu, M. Azkue, H. Camblong, and E. Martinez-Laserna, "Data-Driven Nonparametric Li-Ion Battery Ageing Model Aiming At Learning From Real Operation Data: Holistic Validation With Ev Driving Profiles," in *2020 IEEE Energy Conversion Congress and Exposition (ECCE)*, IEEE, Oct. 2020, pp. 5600–5607. doi: 10.1109/ECCE44975.2020.9235814.
[22] M. Lucu, E. Martinez-Laserna, I. Gandiaga, and H. Camblong, "A critical review on self-adaptive Li-ion battery ageing models," *J Power Sources*, vol. 401, no. May, pp. 85–101, Oct. 2018, doi: 10.1016/j.jpowsour.2018.08.064.
[23] K. Chen *et al.*, "Big data-driven prognostics and health management of lithium-ion batteries:A review," *Renewable and Sustainable Energy Reviews*, vol. 214, p. 115522, May 2025, doi: 10.1016/j.rser.2025.115522.
[24] S. Ansari, A. Ayob, M. S. Hossain Lipu, A. Hussain, and M. H. M. Saad, "Remaining useful life prediction for lithium-ion battery storage system: A comprehensive review of methods, key factors, issues and future outlook," *Energy Reports*, vol. 8, pp. 12153–12185, Nov. 2022, doi: 10.1016/j.egyr.2022.09.043.
[25] M. Lucu *et al.*, "Data-driven nonparametric Li-ion battery ageing model aiming at learning from real operation data - Part B: Cycling operation," *J Energy Storage*, vol. 30, no. March, p. 101410, Aug. 2020, doi: 10.1016/j.est.2020.101410.
[26] M. Lucu *et al.*, "Data-driven nonparametric Li-ion battery ageing model aiming at learning from real operation data – Part A: Storage operation," *J Energy Storage*, vol. 30, no. March, p. 101409, Aug. 2020, doi: 10.1016/j.est.2020.101409.
[27] C. E. Rasmussen and C. K. I. Williams, *Gaussian Processes for Machine Learning*. The MIT Press, 2006.
[28] "BIG LEAP Project." Accessed: Mar. 11, 2025. [Online]. Available: https://bigleapproject.eu/project/
[29] G. Pozzato, A. Allam, and S. Onori, "Lithium-ion battery aging dataset based on electric vehicle real-driving profiles," *Data Brief*, vol. 41, p. 107995, Apr. 2022, doi: 10.1016/j.dib.2022.107995.
[30] J. Olmos, I. Gandiaga, A. Saez-de-Ibarra, X. Larrea, T. Nieva, and I. Aizpuru, "Modelling the cycling degradation of Li-ion batteries: Chemistry influenced stress factors," *J Energy Storage*, vol. 40, no. June, p. 102765, Aug. 2021, doi: 10.1016/j.est.2021.102765.

Presenter Biography

Markel Azkue received his M.Sc in Industrial Engineering from the University of Mondragon in 2020. He joined the Energy Storage and Management unit of Ikerlan Technology Research Centre (BRTA), Spain, in 2016. He obtained his Ph.D. in Applied Engineering with international mention in 2023, focused on Battery SoC and SoH estimation algorithms using AI. He is currently working as a researcher on projects related to lithium-ion batteries. His research interests include machine learning algorithms applied to electrochemical energy storage systems state estimators.